HHS Public Access

Author manuscript

J Magn Reson Imaging. Author manuscript; available in PMC 2021 March 16.

Published in final edited form as:

J Magn Reson Imaging. 2018 October ; 48(4): 1147–1158. doi:10.1002/jmri.26040.

4D Flow MRI Quantification of Mitral and Tricuspid Regurgitation: Reproducibility and Consistency Relative to Conventional MRI

Jennifer F. Feneis, MD[1], **Espoir Kyubwa, PhD**[1], **Kimberly Atianzar, MD**[4], **Joseph Y. Cheng, PhD**[2], **Marcus T. Alley, PhD**[2], **Shreyas S. Vasanawala, MD, PhD**[2], **Anthony N. Demaria, MD**[3], **Albert Hsiao, MD, PhD**[1,*]

[1]Department of Radiology, UC San Diego, La Jolla, California, USA;

[2]Department of Radiology, Stanford, California, USA;

[3]Division of Cardiology, UC San Diego, La Jolla, California, USA;

[4]Department of Cardiovascular Disease, Swedish Heart and Vascular Institute, Seattle, WA

Abstract

Background: In patients with mitral or tricuspid valve regurgitation, evaluation of regurgitant severity is essential for determining the need for surgery. While transthoracic echocardiography is widely accessible, it has limited reproducibility for grading inlet valve regurgitation. Multiplanar cardiac MRI is the quantitative standard but requires specialized local expertise, and is thus not widely available. Volumetric 4D flow MRI has potential for quantitatively grading the severity of inlet valve regurgitation in adult patients.

Purpose: To evaluate the accuracy and reproducibility of volumetric 4D flow MRI for quantification of inlet valvular regurgitation compared to conventional multiplanar MRI, which may simplify and improve accessibility of cardiac MRI.

Study Type: This retrospective, HIPAA-compliant imaging-based comparison study was conducted at a single institution.

Subjects: Twenty-one patients who underwent concurrent multiplanar and 4D flow cardiac MRI between April 2015 and January 2017.

Field Strength/Sequences: 3T; steady-state free-precession (SSFP), 2D phase contrast (2D-PC), and postcontrast 4D flow.

Assessment: We evaluated the intertechnique (4D flow vs. 2D-PC), intermethod (*direct* vs. *indirect* measurement), interobserver and intraobserver reproducibility of measurements of regurgitant flow volume (RFV), fraction (RF), and volume (RVol).

Statistical Tests: Statistical analysis included Pearson correlation, Bland-Altman statistics, and intraclass correlation coefficients.

[*]Address reprint requests to: A.H., Department of Radiology, 9300 Campus Point Dr., #0841, La Jolla, CA 92037-0841. hsiao@ucsd.edu.

Results: There was high concordance between 4D flow and multiplanar MRI, whether using direct or indirect methods of quantifying regurgitation (r = 0.813–0.985). Direct interrogation of the regurgitant jet with 4D flow showed high intraobserver consistency (r = 0.976–0.999) and interobserver consistency (r = 0.861–0.992), and correlated well with traditional indirect measurements obtained as the difference between stroke volume and forward outlet valve flow.

Data Conclusion: 4D flow MRI provides highly reproducible measurements of mitral and tricuspid regurgitant volume, and may be used in place of conventional multiplanar MRI.

Mitral regurgitation (MR) is a common cause of morbidity and mortality, affecting more than 2 million people in the US.[1] With the growing aging population, it is estimated that the prevalence of mitral regurgitation will double by the year 2030.[2] Long-standing regurgitation may lead to progressively more severe regurgitation, ultimately leading to left ventricular failure, pulmonary hypertension, atrial fibrillation, stroke, and death.[3] Early surgical repair of patients with severe primary mitral regurgitation has been shown to improve survival rates, and is recommended even for asymptomatic patients with preserved left ventricular systolic function.[4–6] Therefore, assessment of severity of mitral regurgitation is essential for clinical management, prognosis, and timing of intervention.[5–7] Similarly, assessment of severity of tricuspid regurgitation (TR) is essential for determining the need for surgical management.[6,8,9] At most institutions, the distinction between “moderate” and “severe” regurgitation, currently defined by echocardiography, helps to determine nonsurgical and surgical management.

Transthoracic echocardiography (TTE) is the mainstay of initial diagnosis for assessing mitral and tricuspid regurgitation, but this technique requires the complex task of conceptually integrating multiple imaging features.[10] Even in expert hands, TTE has limited interobserver agreement in distinguishing severe from nonsevere regurgitation, and it may be particularly limited when regurgitant jets are eccentric, multiple, or variable in duration.[11,12] In contrast, quantification of mitral regurgitant volume with multiplanar cardiac magnetic resonance imaging (MRI) shows high reproducibility,[13] better predictive power of patient outcomes for chronic regurgitation,[14] and greater correlation with left ventricular remodeling after surgical repair.[15]

However, multiplanar cardiac MRI is labor-intensive and requires specialized local expertise, limiting its availability.[16] MRI technologists require additional training to become familiar with cardiac anatomy and how to create cardiac imaging planes using multiple oblique localizers. Even if the technologist is able to master the creation of cardiac imaging planes, direct quantification of mitral regurgitation by 2D phase contrast (PC) is challenging, due to dynamic motion of the mitral annulus during systole, and the presence of eccentric regurgitant jets or jets that vary in position throughout systole.[16] Other indirect techniques of quantifying inlet regurgitant volume by multiplanar cardiac MRI are reliant on calculation of ventricular stroke volumes by manually contouring the endocardium in end diastole and end systole, which are prone to error especially at the basal slices.[16–19]

To address the limitations of TTE and multiplanar cardiac MRI, we propose the use of volumetric MRI to quantify regurgitant volume. Over the last few decades, volumetric MRI has been applied by multiple groups to measure cardiac function.[20–22] Several recent

advances, including parallel-imaging, compressed-sensing,[23] combined spatial and temporal acceleration,[24,25] and improvements in visualization and quantification software[26,27] have made this approach feasible in a clinical environment. One element of this approach, 4D flow MRI, has been successfully applied to the evaluation of congenital heart disease (CHD),[28,29] and can provide superior quantitative data for clinical management.[27,30] We hypothesize that volumetric 4D flow MRI may also have potential for quantification of mitral and tricuspid regurgitant volume in adult patients.

4D flow imaging has several advantages over conventional multiplanar cardiac MRI. For example, 4D flow can be prescribed as a single volume acquisition that covers the entire heart, which does not require specialized knowledge of cardiac anatomy and imaging planes for acquisition. In addition, 4D flow may enable direct quantification of regurgitant jets with a single measurement, and could therefore reduce reliance on ventricular endocardial contouring. It is yet uncertain, however, whether 4D flow can be used to measure mitral or tricuspid regurgitation. In contrast to prior work in pediatric patients, it is possible that a free-breathing scan in adults may be more greatly affected by respiratory motion artifact due to increased tidal volumes. Furthermore, when there is “moderate” and “severe” regurgitation, there are correspondingly large pressure gradients between the ventricle and atrium that (may) yield very high-velocity jets. These high-velocity jets have greater spatial and temporal variation, which may challenge current spatial and temporal resolution limits of 4D flow MRI.

The purpose of this study was to evaluate the use of 4D flow MRI for quantification of mitral and tricuspid regurgitant volume with the hypothesis that this technique may have similar accuracy and reproducibility as the reference standard of conventional multiplanar MRI. We further evaluate intermethod (*direct* vs. *indirect*), interobserver and intraobserver reproducibility of mitral and tricuspid regurgitant volume using three quantitative metrics: 1) regurgitant flow volume (RFV), 2) regurgitant fraction (RF), and 3) regurgitant volume (RVol).

Materials and Methods

With Institutional Review Board (IRB) approval and Health Insurance Portability and Accountability Act (HIPAA) compliance, we retrospectively identified all adult patients who underwent concurrent conventional multiplanar MRI and 4D flow volumetric cardiac MRI for quantification of mitral and/or tricuspid valvular regurgitation between April 2015 and January 2017. Informed consent for this retrospective study was waived by the IRB. Twenty-one patients were identified for inclusion, with demographics as listed in Table 1. Out of the 21 patients, 10 had MR, six had TR, and five had both MR and TR. 4D flow image data was successfully acquired in all 21 patients referred for MRI quantification. Complete 2D-PC data were obtained in 18 of the 21 patients. All MRI was performed on a 3T 750 MRI scanner with a 32-channel body array coil (GE Healthcare, Milwaukee, WI).

MRI technical parameters of spatial resolution, temporal resolution, and velocity-encoding speeds (VENC) were customized at the time of image acquisition according to patient body habitus and anticipated severity of inlet valve regurgitation based on prior echocardiographic

results, if available. The parameters range within those utilized in our routine clinical practice, and are listed below.

Multiplanar MRI was performed with a combination of 2D-PC and steady-state free-precession (SSFP) imaging using multiple breath-holds and vector electrocardiographic gating, as prescribed by a board-certified radiologist with ~6 years of experience in cardiovascular MRI (A.H.). SSFP short-axis imaging was performed with the following parameters reported as mean (range): temporal resolution 46 msec (42–54 msec), acquired spatial resolution 1.77 × 1.86 mm (1.33–2.38 × 1.61–2.08 mm), and slice thickness 8 mm. 2D-PC imaging included cross-sectional planes at the level of the aortic valve and pulmonic valve. When mitral and/or tricuspid regurgitation was visualized on SSFP images, 2D-PC imaging was then also obtained along the proximal regurgitant jet in the respective atrium as demonstrated in Fig. 1, with the following parameters: mean temporal resolution 69 msec (range 65–108 msec), acquired spatial resolution 1.96 × 2.26 mm (1.67–1.98 × 1.98–2.5 mm), and slice thickness 8 mm (8–10 mm). Mean VENCs were 200 cm/s (range 150–250 cm/sec) for the aortic and pulmonary valves and 350 cm/sec (150–550 cm/sec) for direct interrogation of regurgitant jets.

4D flow MRI was performed using a Cartesian RF-spoiled gradient recalled echo (GRE)-based sequence with simple four-point flow-encoding, golden angle radial-like Cartesian view ordering with variable density sampling,[31] respiratory self-navigation,[31] compressed-sensing based parallel imaging using respiratory soft-gating,[23,32] and ESPIRiT reconstruction.[33,34] Total acceleration factors were 1.8 in the phase direction and 1.8 in the slice direction. Images were acquired with the following parameters: mean temporal resolution 53 msec (range 37–76 msec), acquired in-plane spatial resolution 1.55 × 1.89 mm (1.22–1.98 × 1.67–2.19 mm), slice thickness 2.5 mm (1.3–3.2 mm), average scan time 11 min 21 sec (8 min 16 sec to 14 min 25 sec), and mean VENC 400 cm/sec (250–550 cm/sec) in all three directions. Initial studies were performed with 0.18 mL/kg of gadofosveset trisodium intravenous contrast (n = 11). When gadofosveset was taken off market after August 2016, 0.3 mL/kg of gadobenate dimeglumine intravenous contrast was used instead (n = 10). Comparison of blood pool-to-myocardial enhancement was quantitatively evaluated by comparing signal intensity of the blood pool (measured in the ascending aorta) to the signal intensity of the basal to mid-interventricular septum in the same phase of the cardiac cycle, using an unpaired t-test.

Multiplanar MRI Analysis

Multiplanar MR images were analyzed with Circle cvi42 v. 5.3.8 (Calgary, AB, Canada). Left and right ventricular volumes were manually contoured at end systole and end diastole from base to apex on SSFP short-axis stack images in order to calculate biventricular stroke volumes (in mL), including trabeculations and papillary muscles with the blood pool in both phases of the cardiac cycle.[16] Aortic and pulmonary outputs were measured by segmenting the vessel lumen throughout the cardiac cycle. Background phase-error in 2D-PC was corrected with local soft-tissue background-correction. When 2D-PC cross-sections of the regurgitant jet were available, direct measurements of the regurgitant flow volume were performed by segmenting the flow jet during systolic phases where the jet was present.

4D Flow Volumetric MRI Analysis

4D flow analysis with background phase correction was performed on Arterys Cardio DL 2.2 (San Francisco, CA) by two readers of varied levels of expertise; one reader was a senior level radiology resident (J.F.), and the second was a cardiovascular radiologist with 6 years of cardiac imaging experience (A.H.). In a manner similar to conventional multiplanar imaging, each reader independently measured blood flow through the aortic root and main pulmonary artery in duplicate, at least 5 mm apart. Each reader also measured mitral and/or tricuspid regurgitant flow volumes by directly interrogating the regurgitant jet throughout the cardiac cycle at multiple distances from the valve plane, at least 5 mm apart, avoiding regions of velocity-aliasing and segments of severe signal dephasing (Fig. 1). The readers were blinded to each other's results.

Calculations of Regurgitant Volume

Three metrics of quantitating regurgitant volume were included in this analysis (RFV, RF, and Rvol), recognizing that practitioners of cardiac MRI may differ in their preference to use one metric over another. RFV (in L/min) may be either measured directly by interrogating the regurgitant jet with phase-contrast (either 2D-PC or 4D flow) imaging, or indirectly by subtracting aortic forward flow from the cardiac output measured from SSFP imaging. Direct RFV was performed solely from phase-contrast flow measurements, without any measurement of cardiac stroke volume. Indirect measurements of regurgitant volume were computed as:

$$RFV_{indirect} = (SV \times HR) - Q_{forward} \quad (1)$$

where SV is the stroke volume from SSFP imaging, HR is the heart rate, and $Q_{forward}$ is the forward output from the outlet valve.

RF and RVol were normalized against cardiac output and heart rate, respectively. Calculations of regurgitant fraction (in percentage, %), for direct measurements were computed as:

$$RF_{direct} = RFV_{direct}/\left(RFV_{direct} + Q_{forward}\right) \quad (2)$$

Calculations of regurgitant fraction for indirect measurements were normalized against measured cardiac outputs from SSFP imaging:

$$RF_{indirect} = RFV_{indirect}/(SV \times HR) \quad (3)$$

Regurgitant volume (in mL/beat) was computed as the regurgitant flow volume divided by the heart rate, whether direct or indirect methods of calculating RFV were used:

$$RVol = RFV/HR \times 1,000 \quad (4)$$

Statistical Analysis

Intertechnique, intermethod, interobserver, and intraobserver reliability were calculated using Pearson correlation analysis and Bland-Altman statistics in Prism (v. 7, GraphPad Software, La Jolla, CA). Reliability was also calculated with an intraclass correlation (ICC), a two-way random effects absolute agreement model[35] using custom-built script in MatLab (MathWorks, Natick, MA). Pearson correlation (r) was considered poor for values between 0.25–0.50, moderate to good for $r = 0.50–0.75$, and very good to excellent for $r = 0.75–1.00$. Variability between measurements was measured by the span of the limits of agreement in the Bland-Altman statistics. Reliability was considered to be poor for ICC values below 0.40, fair for values between 0.41 and 0.59, good for values between 0.60 and 0.74, and excellent for values between 0.75 and 1.00. Statistics to compare differences in reliability between groups were calculated using the Wilcoxon matched-pairs signed rank test. $P < 0.05$ was considered statistically significant.

Results

Patients included in this study exhibited a wide range of severity of mitral and tricuspid regurgitation. With 4D flow, direct measurements of regurgitant flow volume ranged from 0.6–6.4 L/min (mean 2.5 L/min) for mitral regurgitation, and 0.7–16.3 L/min (mean 5.3 L/min) for tricuspid regurgitation. 4D flow direct measurements of regurgitant fraction ranged from 5–58% (mean 29%) for mitral regurgitation and 16–78% (mean 42%) for tricuspid regurgitation. With conventional imaging, direct measurements of regurgitant volume ranged from 0.6–5.3 L/min (mean 2.9 L/min) for mitral regurgitation, and 3.2–11.4 L/min (mean 4.9 L/min) for tricuspid regurgitation. Of note, direct 2D-PC of the tricuspid regurgitant jet was not acquired in the patient who demonstrated the most severe tricuspid regurgitation (16.3 L/min) by 4D flow. 2D-PC direct measurements of regurgitant fraction ranged from 13–54% (mean 34%) for mitral regurgitation and 17–60% (mean 46%) for tricuspid regurgitation.

In addition to the wide range of severity of regurgitation, the regurgitant jets also demonstrated a wide range of morphologies, as depicted in Fig. 2 with their corresponding flow curves. Note that the duration of valvular regurgitation contributes greatly to the total regurgitant volume.

Eleven patients had MRIs performed with gadofosveset trisodium intravenous contrast material, with a mean ratio of signal intensity of the blood pool relative to the interventricular septal myocardium of 1.35 (range 1.21–1.60). Ten patients had MRIs performed with gadobenate dimeglumine intravenous contrast material, with a mean ratio of 1.41 (range 1.19–1.94). Utilizing an unpaired t-test, there was no statistically significant difference in these values ($P = 0.4637$, 95% CI −0.2283 to 0.1081).

Intertechnique Agreement Between 4D flow and 2D-PC MRI

We first compared the consistency of mitral regurgitation measurements between 4D flow and 2D-PC techniques, which demonstrated high concordance, as depicted in Fig. 3 and Table 2. There was slightly higher intertechnique consistency ($P < 0.002$) in the

quantification of mitral regurgitant volume using the indirect method (r = 0.971 for RFV, r = 0.933 for RF, r = 0.952 for Rvol) compared to the direct method (r = 0.813 for RFV, r = 0.868 for RF, r = 0.793 for Rvol). This is depicted by the narrow 95% confidence interval in the linear correlation between volumetric 4D flow and multiplanar 2D-PC shown in Fig. 3 and narrower Bland-Altman (B-A) limits of agreement for the direct method (Table 2).

We next compared the consistency of tricuspid regurgitation measurements between 4D flow and 2D-PC techniques, which also demonstrated high concordance, as depicted in Fig. 4 and Table 2. Concordance between techniques was even higher for direct quantification of tricuspid flow volume (r = 0.985; ICC = 0.982), as compared to mitral regurgitant flow volume (r = 0.813; ICC = 0.804), and with even narrower B-A limits of agreement (Table 2).

Intermethod Agreement Between Direct and Indirect Methods

We then compared the consistency of direct vs. indirect methods of quantifying mitral regurgitation for 4D flow and for 2D-PC, separately (Table 3, Fig. 5, black). Although the indirect approach is more widely used clinically, the direct method is also technically feasible, especially with 4D flow imaging. There was very good to excellent agreement between methods for regurgitant flow volume (r = 0.794; ICC = 0.654 for 4D flow and r = 0.868; ICC = 0.857 for 2D-PC), regurgitant fraction (r = 0.819; ICC = 0.777 for 4D flow and r = 0.902; ICC = 0.904 for 2D-PC) and regurgitant volume (r = 0.718; ICC = 0.627 for 4D flow and r = 0.831; ICC = 0.834 for 2D-PC).

We similarly compared the consistency of direct vs. indirect methods for quantifying tricuspid regurgitation for 4D flow and for 2D-PC (Table 3, Fig. 5, red). 4D flow demonstrated even higher intermethod consistency than 2D-PC for tricuspid regurgitant fraction (r = 0.950; ICC = 0.903 for 4D flow and r = 0.846; ICC = 0.840 for 2D-PC) and regurgitant volume (r = 0.920; ICC = 0.831 for 4D flow and r = 0.832; ICC = 0.796 for 2D-PC).

Interobserver and Intraobserver Agreement Between and Within Reader 1 and Reader 2

Finally, we assessed the interobserver and intraobserver reliability for direct quantification of inlet valve regurgitation with 4D flow, as depicted in Table 4 and Fig. 6. Interobserver analysis demonstrated very good to excellent reproducibility between readers for quantification of mitral regurgitant flow volume (r = 0.929 for direct, r = 0.877 for indirect), and fraction (r = 0.861 for direct and r = 0.838 for indirect). Interobserver reproducibility was even higher for quantification of tricuspid regurgitation with 4D flow regurgitant flow volume (r = 0.992 for direct, r = 0.994 for indirect), and fraction (r = 0.975 for direct and r = 0.968 for indirect). Intraobserver analysis also demonstrated very high internal consistency for each reader for quantification of mitral and tricuspid regurgitant flow volume, fractions, and volumes, also depicted in Table 4. For example, Readers 1 and 2 demonstrated similarly high internal consistency for direct quantification of mitral regurgitant flow volume (r = 0.988 for Reader 1 and r = 0.986 for Reader 2) and tricuspid regurgitant flow volume (r = 0.999 for Reader 1 and r = 0.998 for Reader 2).

Discussion

We have shown that quantification of mitral and tricuspid regurgitation by 4D flow MRI is highly reproducible and consistent across multiple methods of measurement, with high concordance to multiplanar MRI. Additionally, we find that measurement of regurgitant volume using either direct or indirect techniques yields equivalent results, whether performed with 4D flow or 2D-PC. Finally, we show that 4D flow volumetric technique has excellent interobserver and intraobserver reliability for quantification of regurgitant fraction and volume. These observations highlight the opportunity to apply 4D flow MRI to simplify and improve the robustness of quantification of valvular regurgitation. Given limited reproducibility of TTE, 4D flow MRI may provide a more reliable and accessible method for stratifying patients with severe regurgitation for subsequent mitral or tricuspid valve surgery.

Our data show that although intertechnique concordance was high for direct quantification of mitral regurgitant flow volume, it was even higher for direct quantification of tricuspid regurgitant flow volume. Interobserver reproducibility was also higher for direct quantification of tricuspid regurgitation. This may be a reflection of the differing morphologies of tricuspid vs. mitral regurgitant jets. The tricuspid regurgitant jets tend to be more laminar than the mitral regurgitant jets, and much easier to perform direct measurements using either 4D flow or 2D-PC. In contrast, the mitral regurgitant jets may change orientation and position considerably during systole. This may impair the ability to perform a direct measurement with a static imaging plane with 2D-PC.

One advantage of 4D flow MRI is that this technique facilitates direct measurement of regurgitant volume, complementing the indirect measurements that are typically performed clinically by subtracting aortic forward flow from left ventricular stroke volume. This direct measurement does not require additional segmentation of ventricular volumes to determine stroke volume. While in expert hands, ventricular volumetry is highly reproducible, this may be difficult to achieve in practice outside of specialized academic centers.[17,18] Basal segmentations in particular are subject to greater error.[18] Alternatively, since different imaging strategies may be susceptible to different sources of artifact or measurement error, using both direct and indirect methods of measurement may provide redundancy to maximize robustness of MRI, and ensure patients are appropriately classified as having “severe” or “nonsevere” regurgitation. In practice, use of 4D flow MRI instead of conventional phase contrast provides the opportunity to perform both direct and indirect quantification of inlet valve regurgitation, without the cost of direct physician oversight of plane prescription and scan time.

Current guidelines for management of mitral regurgitation are based on the presence or absence of severe regurgitation by echocardiography.[5] However, it is unclear at present what “severity” of regurgitation leads to the downstream consequences of irreversible left ventricular failure. Similarly, it is unclear whether concurrent aortic regurgitation yields similar outcomes as isolated mitral regurgitation. An earlier study by Myerson et al demonstrated poor 5-year survival outcome of patients with regurgitant volume of greater than 55 mL without mitral valve surgery.[36] They therefore suggest a mitral regurgitant

volume of 55 mL or a regurgitant fraction of 40% as a threshold for surgery for asymptomatic patients.[36] However, the MRI thresholds for severe mitral regurgitation that most closely match echocardiography are uncertain, and in one study regurgitant fraction thresholds for mild, moderate, moderate to severe, and severe regurgitation were reported to be ≤15%, 16–25%, 26–48%, and >48%, respectively.[37]

In our study, one-third of our patients satisfied the 55 mL regurgitant volume threshold. With 4D flow MRI, it may now be possible to further evaluate the long-term outcomes of patients considered for surgery, at different quantitative thresholds of valvular regurgitation. With a precise quantitative technique like 4D flow, a study such as this would require fewer numbers of patients to undertake and provide prognostic information to guide surgical decision-making.

We also observed in our study the presence of turbulent regurgitant flow jets in some patients with severe mitral regurgitation. At present, it is unclear whether turbulent flow itself has negative prognostic implications, but it is known that turbulent flow creates MRI signal voids in phase-contrast imaging,[38,39] which negatively affect the direct quantification of blood flow.[19,40] Future work with turbulent flow imaging may further improve the reproducibility of 4D flow measurements and prognostication.

We have identified a few limitations of this study. The study was conducted at a single site with extensive experience with both multiplanar MRI and volumetric 4D flow MRI for evaluation of structural heart abnormalities. It may not be possible at all sites to perform multiplanar MRI due to lack or unavailability of local specialized expertise. In addition, while 4D flow MRI has recently become a clinical product by one MRI vendor, it is not yet widely available on all MRI platforms, and it is unclear if other platforms or analysis software can obtain measurements of similar accuracy or reproducibility. However, the present work may provide a template for future work on other platforms and analysis software.

Additionally, this study was designed to specifically focus on comparison between MRI techniques, without comparison with echocardiography. Prior studies have explored the reliability and accuracy of valve regurgitation quantitation between echocardiography and multiplanar cardiac MRI, which have shown multiplanar cardiac MRI to have high reproducibility,[13] better predictive power of patient outcomes for chronic regurgitation,[14] and greater correlation with left ventricular remodeling after surgical repair.[15] To our knowledge, there are no similar studies directly comparing echocardiography with 4D flow MRI. The present work, in combination with these prior studies, may serve as a basis for such future evaluation.

In conclusion, this study offers technical evidence supporting the application of 4D flow cardiac MRI to quantify mitral and tricuspid regurgitant volume. 4D flow may simplify evaluation of structural cardiac abnormalities with MRI by reducing the workload and expertise required of the technologist performing the MRI, eliminating the need for on-site physician expertise, and reducing the need for postprocessing of ventricular stroke volumes in order to quantify inlet valve regurgitation. If used in combination with existing indirect

measurements, it can provide even greater redundancy and robustness to quantification of regurgitant volume to help guide clinical management of these patients.

Funding Sources and Conflict of Interest

E. Kyubwa is supported by the Howard Hughes Medical Institute Gilliam Fellowship and the University of California, San Diego Medical Scientist Training Program T32 GM007198-40. M.T. Alley discloses research funding from General Electric and is a consultant to Arterys Inc. S.S. Vasanawala is involved with research collaboration with General Electric, is a founder and consultant to Arterys Inc, and has a research grant from Bayer AG. A. Hsiao is founder and consultant to Arterys, Inc, and has a research grant from GE Healthcare.

References

1. Enriquez-Sarano M, Akins CW, Vahanian A. Mitral regurgitation. Lancet 2009;373:1382–1394. [PubMed: 19356795]
2. De Marchena E, Badiye A, Robalino G, et al. Respective prevalence of the different Carpentier classes of mitral regurgitation: A stepping stone for future therapeutic research and development. J Card Surg 2011:385–392. [PubMed: 21793928]
3. Ling LH, Enriquez-Sarano M, Seward JB, et al. Clinical outcome of mitral regurgitation due to flail leaflet. N Engl J Med 1996;335:1417–1423. [PubMed: 8875918]
4. Kang D-H, Kim JH, Rim JH, et al. Comparison of early surgery vs. conventional treatment in asymptomatic severe mitral regurgitation. Circulation 2009;119:797–804. [PubMed: 19188506]
5. Nishimura RA, Otto CM, Bonow RO, et al. 2017 AHA/ACC Focused Update of the 2014 AHA/ACC Guideline for the Management of Patients With Valvular Heart Disease. A Report of the American College of Cardiology/American Heart Association Task Force on Clinical Practice Guidelines. Circulation 2017;135:e1159–e1195. [PubMed: 28298458]
6. Nishimura RA, Otto CM, Bonow RO, et al. 2014 AHA/ACC guideline for the management of patients with valvular heart disease: Executive summary: A report of the American College of Cardiology/American Heart Association Task Force on practice guidelines. J Am Coll Cardiol 2014;63:2438–2488. [PubMed: 24603192]
7. Liu B, Edwards NC, Ray S, Steeds RP. Timing surgery in mitral regurgitation: defining risk and optimising intervention using stress echocardiography. Echo Res Pract 2016;3:R45–R55. [PubMed: 27737905]
8. Nath J, Foster E, Heidenreich PA. Impact of tricuspid regurgitation on long-term survival. J Am Coll Cardiol 2004;43:405–409. [PubMed: 15013122]
9. Rodés-Cabau J, Taramasso M, O'Gara PT. Diagnosis and treatment of tricuspid valve disease: current and future perspectives. Lancet 2016: 2431–2442. [PubMed: 27048553]
10. Zoghbi WA, Adams D, Bonow RO, et al. Recommendations for noninvasive evaluation of native valvular regurgitation: a report from the American Society of Echocardiography developed in collaboration with the Society for Cardiovascular Magnetic Resonance. J Am Soc Echocardiogr 2017;30:303–371. [PubMed: 28314623]
11. Enriquez-Sarano M, Miller FA, Hayes SN, Bailey KR, Tajik AJ, Seward JB. Effective mitral regurgitant orifice area: Clinical use and pitfalls of the proximal isovelocity surface area method. J Am Coll Cardiol 1995;25:703–709. [PubMed: 7860917]
12. Biner S, Rafique A, Rafii F, et al. Reproducibility of proximal isovelocity surface area, vena contracta, and regurgitant jet area for assessment of mitral regurgitation severity. JACC Cardiovasc Imaging 2010; 3:235–243. [PubMed: 20223419]
13. Cawley PJ, Hamilton-Craig C, Owens DS, et al. Prospective comparison of valve regurgitation quantitation by cardiac magnetic resonance imaging and transthoracic echocardiography. Circ Cardiovasc Imaging 2013;6:48–57. [PubMed: 23212272]
14. Harris AW, Krieger EV, Kim M, et al. Cardiac Magnetic Resonance Imaging Vs. Transthoracic Echocardiography for Prediction of Outcomes in Chronic Aortic or Mitral Regurgitation. Am J Cardiol 2017;119:1074–1081. [PubMed: 28153348]

15. Uretsky S, Gillam L, Lang R, et al. Discordance between echocardiography and MRI in the assessment of mitral regurgitation severity: A prospective multicenter trial. J Am Coll Cardiol 2015;65:1078–1088. [PubMed: 25790878]
16. Krieger EV, Lee J, Branch KR, et al. Quantitation of mitral regurgitation with cardiac magnetic resonance imaging: a systematic review. Heart 2016;102:1–1870. [PubMed: 26660869]
17. Suinesiaputra A, Bluemke DA, Cowan BR, et al. Quantification of LV function and mass by cardiovascular magnetic resonance: multi-center variability and consensus contours. J Cardiovasc Magn Reson 2015;17:63. [PubMed: 26215273]
18. Karamitsos T, Hudsmith L, Selvanayagam J, Neubauer S, Francis J. Operator induced variability in left ventricular measurements with cardiovascular magnetic resonance is improved after training. J Cardiovasc Magn Reson 2007;9:777–783. [PubMed: 17891615]
19. Buonocore MH, Bogren H. Factors influencing the accuracy and precision of velocity-encoded phase imaging. Magn Reson Med 1992;26:141–154. [PubMed: 1625560]
20. Markl M, Frydrychowicz A, Kozerke S, Hope M, Wieben O. 4D flow MRI. J Magn Reson Imaging 2012;36:1015–1036. [PubMed: 23090914]
21. Pelc NJ, Herfkens RJ, Shimakawa A, Enzmann DR. Phase contrast cine magnetic resonance imaging. Magn Reson Q 1991;7:229–254. [PubMed: 1790111]
22. Kozerke S, Tsao J, Razavi R, Boesiger P. Accelerating cardiac cine 3D imaging using k-t BLAST. Magn Reson Med 2004;52:19–26. [PubMed: 15236362]
23. Vasanawala SS, Alley MT, Hargreaves BA, Barth RA, Pauly JM, Lustig M. Improved pediatric MR imaging with compressed sensing. Radiology 2010;256:607–616. [PubMed: 20529991]
24. Greil GF, Germann S, Kozerke S, et al. Assessment of left ventricular volumes and mass with fast 3D cine steady-state free precession k-t space broad-use linear acquisition speed-up technique (k-t BLAST). J Magn Reson Imaging 2008;27:510–515. [PubMed: 18183581]
25. Tsao J, Boesiger P, Pruessmann KP. k-t BLAST and k-t SENSE: dynamic MRI with high frame rate exploiting spatiotemporal correlations. Magn Reson Med 2003;50:1031–1042. [PubMed: 14587014]
26. Hsiao A, Lustig M, Alley MT, Murphy MJ, Vasanawala SS. Evaluation of valvular insufficiency and shunts with parallel-imaging compressed-sensing 4D phase-contrast MR imaging with stereoscopic 3D velocity-fusion volume-rendered visualization. Radiology 2012;265:87–95. [PubMed: 22923717]
27. Hsiao A, Lustig M, Alley MT, et al. Rapid pediatric cardiac assessment of flow and ventricular volume with compressed sensing parallel imaging volumetric cine phase-contrast MRI. AJR Am J Roentgenol 2012; 198:W250–259. [PubMed: 22358022]
28. Lawley CM, Broadhouse KM, Callaghan FM, Winlaw DS, Figtree GA, Grieve SM. 4D flow magnetic resonance imaging: role in pediatric congenital heart disease. Asian Cardiovasc Thorac Ann 2018;26:28–37 [PubMed: 28185475]
29. Vasanawala SS, Hanneman K, Alley MT, Hsiao A. Congenital heart disease assessment with 4D flow MRI. J Magn Reson Imaging 2015:1–17.
30. Hsiao A, Alley MT, Massaband P, Herfkens RJ, Chan FP, Vasanawala SS. Improved cardiovascular flow quantification with time-resolved volumetric phase-contrast MRI. Pediatr Radiol 2011;41:711–720. [PubMed: 21221566]
31. Cheng JY, Hanneman K, Zhang T, et al. Comprehensive motion-compensated highly accelerated 4D flow MRI with ferumoxytol enhancement for pediatric congenital heart disease. J Magn Reson Imaging 2015:1355–1368. [PubMed: 26646061]
32. Cheng JY, Zhang T, Ruangwattanapaisarn N, et al. Free-breathing pediatric MRI with nonrigid motion correction and acceleration. J Magn Reson Imaging 2015;42:407–420. [PubMed: 25329325]
33. Feng L, Srichai MB, Lim RP, et al. Highly accelerated real-time cardiac cine MRI using k-t SPARSE-SENSE. Magn Reson Med 2013;70:64–74. [PubMed: 22887290]
34. Uecker M, Lai P, Murphy MJ, et al. ESPIRiT—an eigenvalue approach to autocalibrating parallel MRI: Where SENSE meets GRAPPA. Magn Reson Med 2013;1001:990–1001.
35. McGraw KO, Wong SP. Forming inference about some intraclass correlation coefficients. Psychol Methods 1996;1:30–46.

36. Myerson SG, D'Arcy J, Christiansen JP, et al. Determination of clinical outcome in mitral regurgitation with cardiovascular magnetic resonance quantification. Circulation 2016;133:2287–2296. [PubMed: 27189033]

37. Gelfand EV, Hughes S, Hauser TH, et al. Severity of mitral and aortic regurgitation as assessed by cardiovascular magnetic resonance: optimizing correlation with Doppler echocardiography. J Cardiovasc Magn Reson 2006;8:503–507. [PubMed: 16755839]

38. Gao JH, Gore JO. Turbulent flow effects on NMR imaging: measurement of turbulent intensity. Med Phys 1991;18:1045–1051. [PubMed: 1961145]

39. Sechtem U, Pflugfelder PW, Cassidy MM, et al. Mitral or aortic regurgitation: quantification of regurgitant volumes with cine MR imaging. Radiology 1988;167:425–430. [PubMed: 3357951]

40. Hsiao A, Alley MT, Massaband P, Herfkens RJ, Chan FP, Vasanawala SS. Improved cardiovascular flow quantification with time-resolved volumetric phase-contrast MRI. Pediatr Radiol 2011; 41:711–720. [PubMed: 21221566]

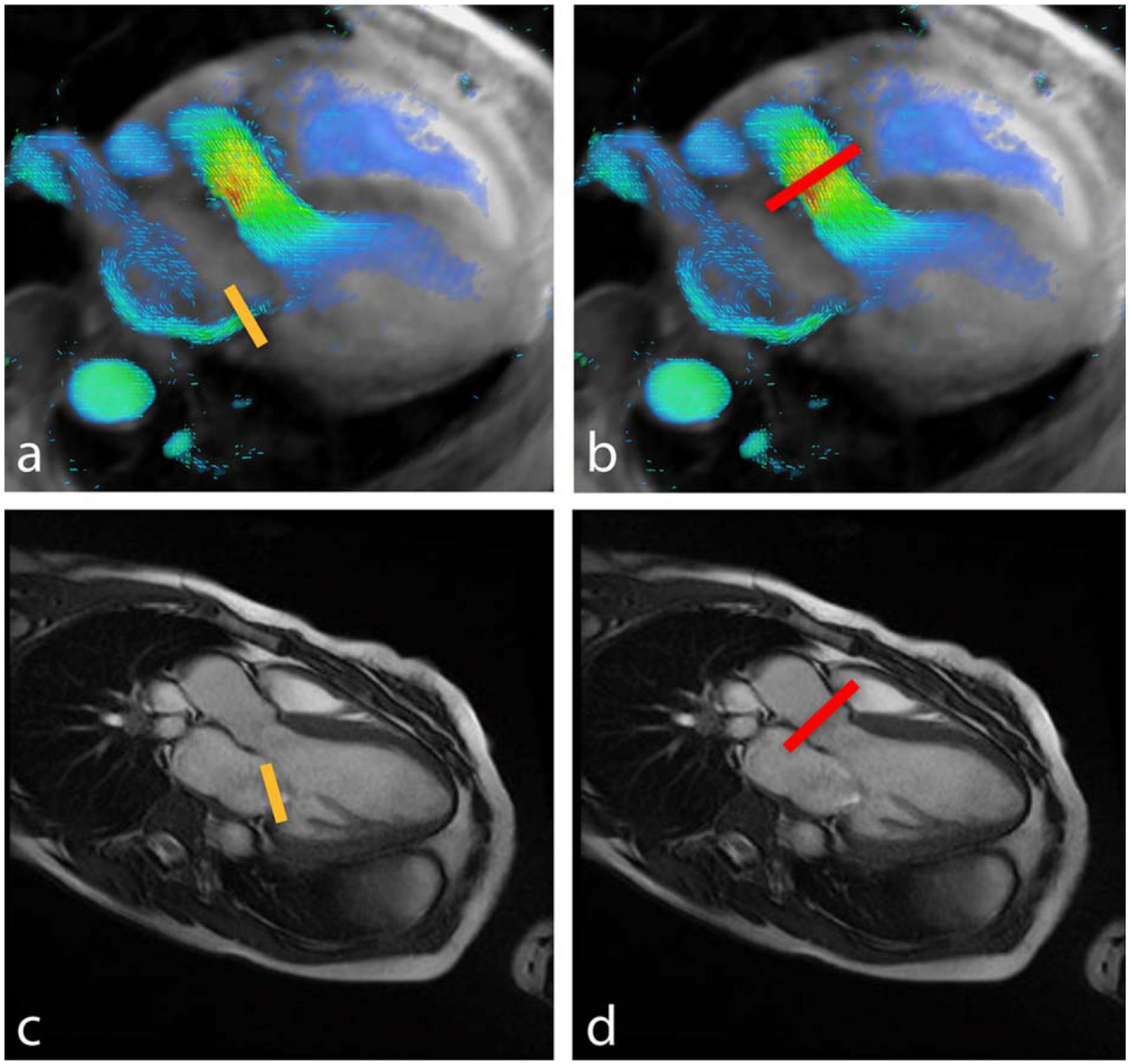

FIGURE 1:
Quantification of mitral regurgitant volume by 4D flow (top) and planar MRI (bottom). Methods of measurement include direct interrogation of the regurgitant jet (left, yellow lines) or indirect quantification by subtracting aortic flow (right, red lines) from stroke volume.

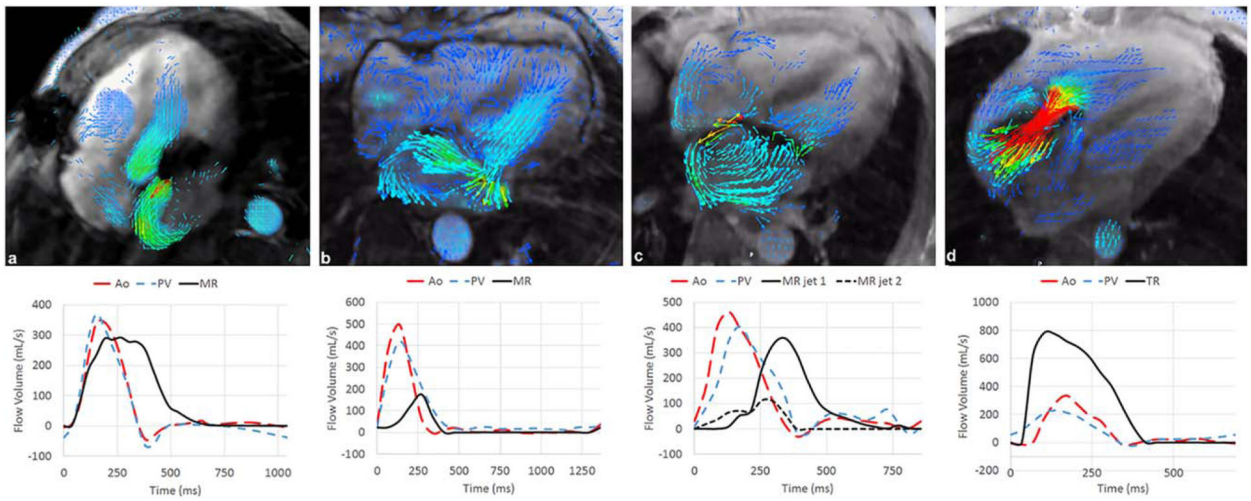

FIGURE 2:

Morphologies and waveforms of mitral and tricuspid regurgitation visualized with 4D flow MRI. Multiple morphologies of mitral regurgitation were identified, characterized as **(a)** large-orifice eccentric, **(b)** complex, broad-based, **(c)** narrow-orifice eccentric regurgitation with a long segment of proximal turbulent signal loss. In addition, high-velocity, wide-orifice tricuspid regurgitation is also shown **(d)**. Flow curves on the bottom highlight the duration and temporal relationship of mitral regurgitation relative to the aortic and pulmonary outflow.

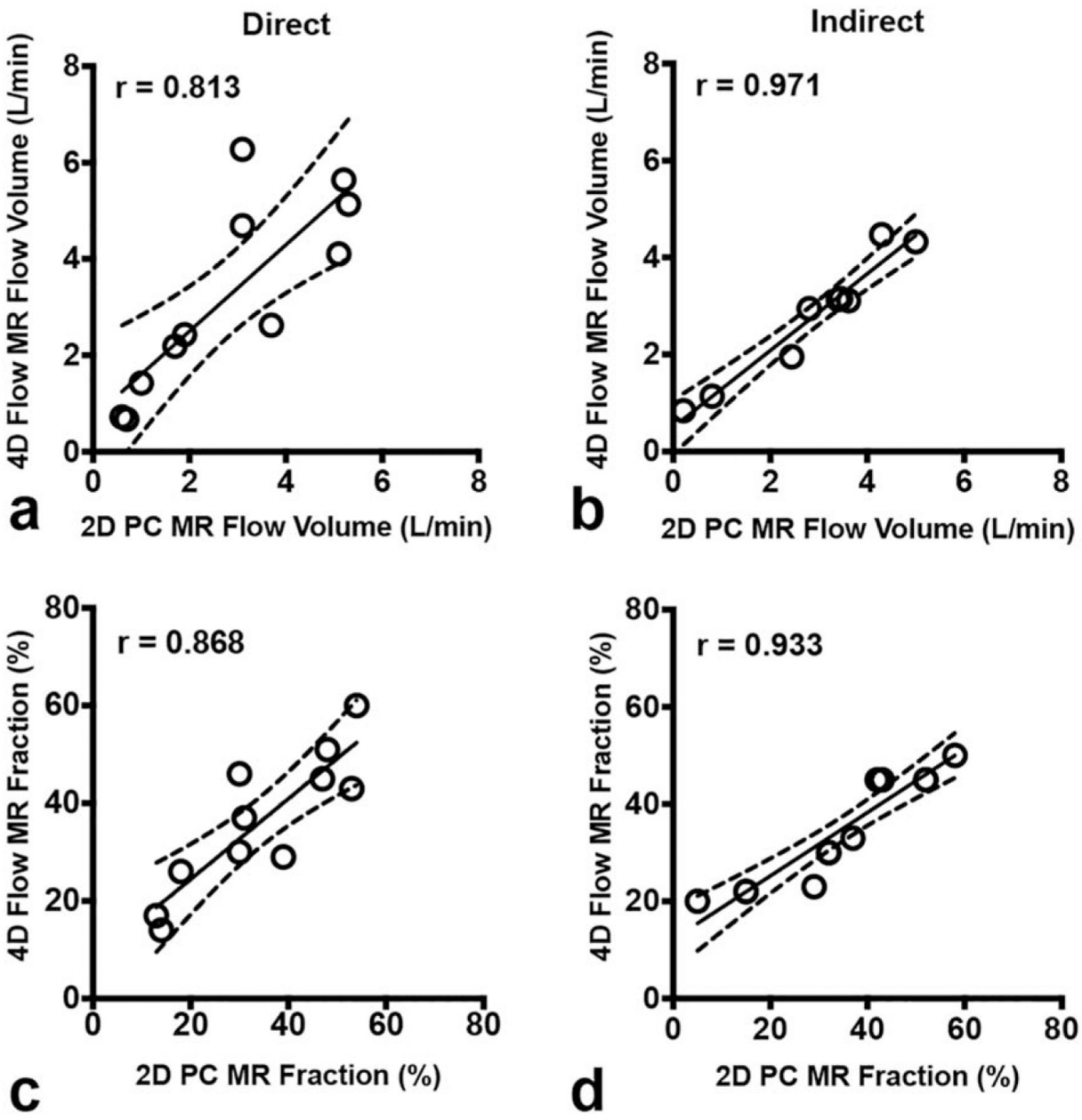

FIGURE 3:

Comparison of 4D flow vs. 2D-PC for quantification of MR. Scatterplots demonstrate high consistency for both direct (left panels) and indirect (right panels) methods of quantifying regurgitant flow volume (top panels) and regurgitant fraction (bottom panels). The solid line is the line of best fit using least squares method. The dashed lines indicate the asymptotic 95% confidence intervals (CI). *r* = Pearson correlation coefficient.

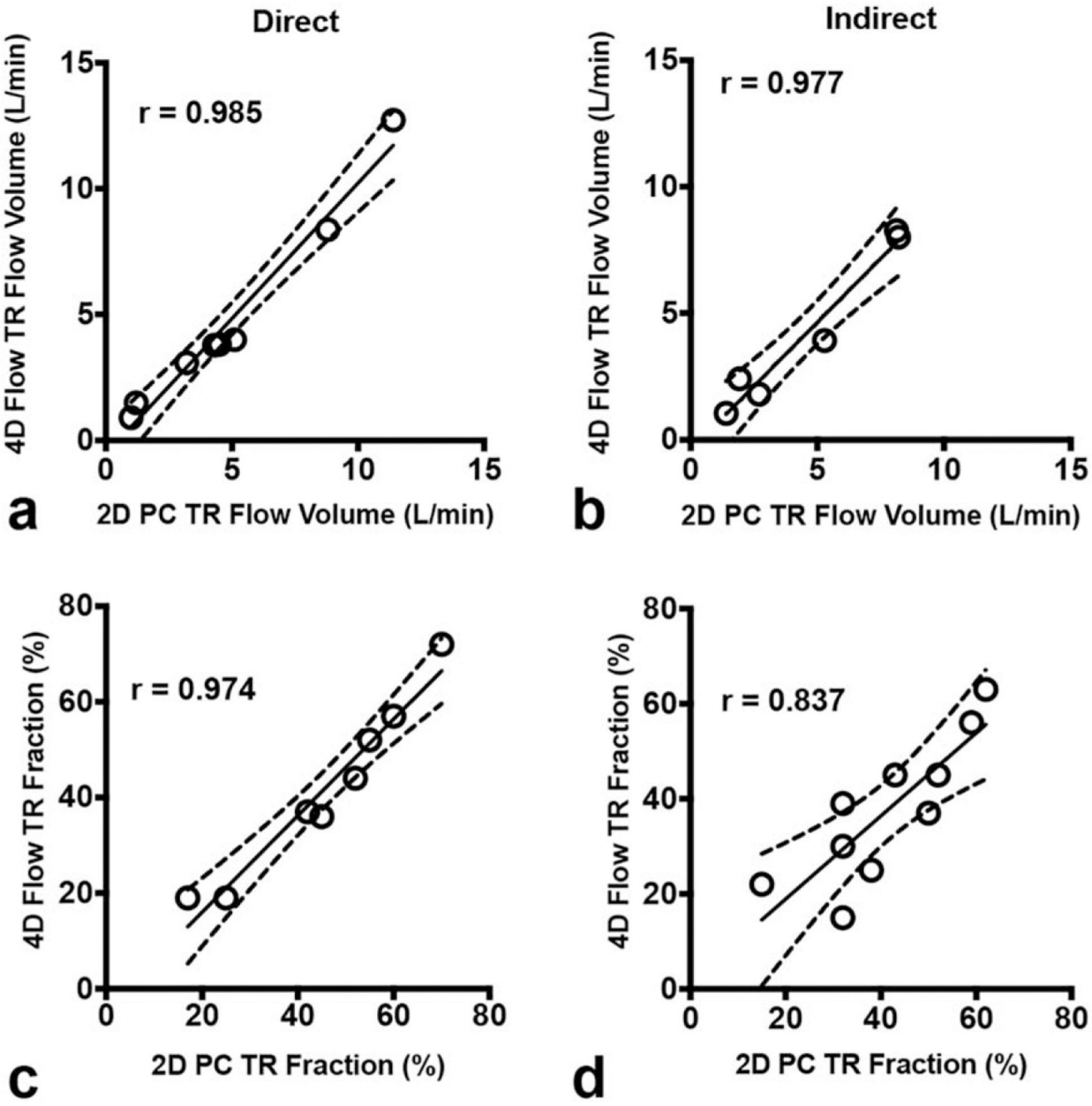

FIGURE 4:

Comparison of 4D flow vs. 2D-PC for quantification of TR. Scatterplots demonstrate high consistency for both direct (left panels) and indirect (right panels) methods of quantifying regurgitant flow volume (top panels) and regurgitant fraction (bottom panels). The solid line is the line of best fit using least squares method. The dashed lines indicate the asymptotic 95% confidence intervals (CI). r = Pearson correlation coefficient.

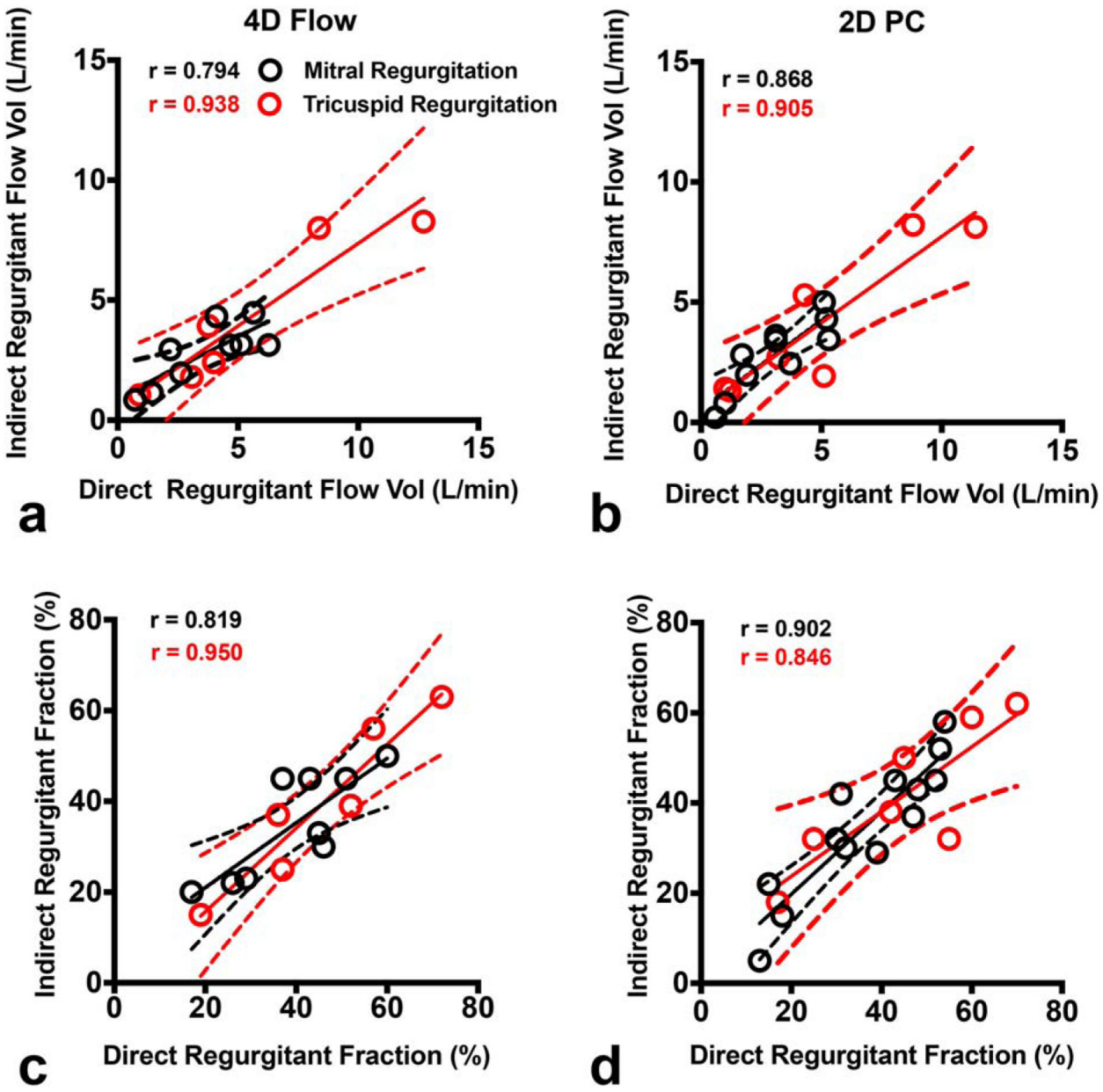

FIGURE 5:

Comparison of direct and indirect methods for quantification of regurgitation. Scatterplots of MR (black) and TR (red) demonstrate high agreement between direct and indirect methods of quantifying regurgitant flow volume (top panels) and regurgitant fraction (bottom panels) with both 4D flow (left panels) and 2D-PC (right panels) MRI. The solid line is the line of best fit using least squares method. The dashed lines indicate the asymptotic 95% confidence intervals (CI). *r* = Pearson correlation coefficient.

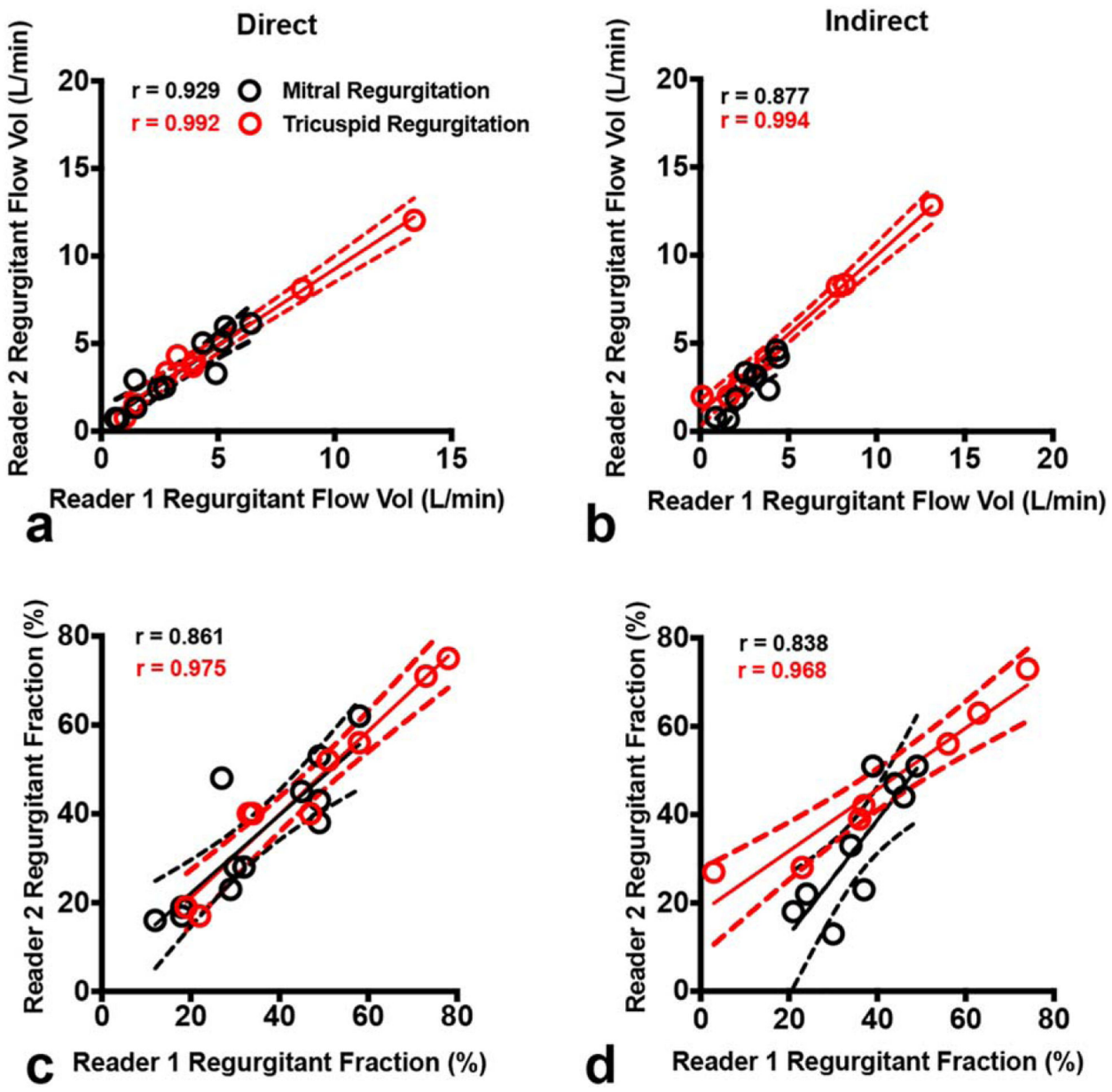

FIGURE 6:

Interobserver consistency of quantitative measurements. Scatterplots of MR (black) and TR (red) demonstrate high reproducibility between Readers 1 and 2 for both direct (left panels) and indirect (right panels) methods in quantifying regurgitant flow volume (top panels) and regurgitant fraction (bottom panels). The solid line is the line of best fit using least squares method. The dashed lines indicate the asymptotic 95% confidence intervals (CI). *r* = Pearson correlation coefficient.

TABLE 1.

Characteristics of Study Population

Patient demographics	**Mean (Range)**
Total patients (male:female)	21 (10:11)
Age (years)	54.1 (21–83)
Weight (kg)	74.5 (45.4–110.2)
Height (cm)	169.6 (148–193)
BSA (m^2)[a]	1.86 (1.4–2.36)
Heart rate (bpm)	65.3 (44–90)

[a]BSA = body surface area, calculated using the Mosteller method.

TABLE 2.

Intertechnique Consistency for Quantifying Regurgitant Volume

	Mitral Regurgitation			Tricuspid Regurgitation		
	Pearson	**95% Limits of agreement**	**ICC**	**Pearson**	**95% Limits of agreement**	**ICC**
Regurgitant flow volume (L/min)						
Direct	0.813	(−2.72, 1.90)	0.804	0.985	(−1.27, 1.61)	0.982
Indirect	0.971	(−0.76, 0.98)	0.953	0.977	(−0.96, 1.70)	0.973
Regurgitant fraction (%)						
Direct	0.868	(−16.85, 13.03)	0.870	0.974	(−4.35, 11.85)	0.956
Indirect	0.933	(−13.41, 14.41)	0.878	0.837	(−12.85, 20.43)	0.785
Regurgitant volume (mL/beat)						
Direct	0.793	(−39.50, 25.68)	0.771	0.972	(−20.67, 27.42)	0.971
Indirect	0.952	(−13.13, 14.24)	0.949	0.959	(−16.72, 28.72)	0.955

Data in parentheses are Bland-Altman 95% limits of agreement.

ICC = interclass correlation coefficient, 2-way random effects absolute agreement model.

TABLE 3.

Intermethod (Direct vs. Indirect) Consistency for Quantifying Regurgitant Volume

	Mitral Regurgitation			Tricuspid Regurgitation		
	Pearson	**95% Limits of agreement**	**ICC**	**Pearson**	**95% Limits of agreement**	**ICC**
Regurgitant flow volume (L/min)						
2D PC	0.868	(−1.44, 1.98)	0.857	0.905	(−2.47, 4.18)	0.870
4D flow	0.794	(−1.56, 3.28)	0.654	0.938	(−2.16, 4.63)	0.864
Regurgitant fraction (%)						
2D PC	0.902	(−11.1, 13.8)	0.904	0.846	(−16.5, 23.0)	0.840
4D Flow	0.819	(−10.6, 19.7)	0.777	0.950	(−5.14, 17.8)	0.903
Regurgitant volume (mL/beat)						
2D PC	0.831	(−23.0, 29.9)	0.834	0.832	(−43.8, 69.8)	0.796
4D Flow	0.718	(−25.1, 48.0)	0.627	0.920	(−30.4, 67.4)	0.831

Data in parentheses are Bland-Altman 95% limits of agreement.

ICC = interclass correlation coefficient, 2-way random effects absolute agreement model.

TABLE 4.

Interobserver and Intraobserver Consistency for Quantifying Regurgitant Volume by 4D Flow

	Mitral Regurgitation			Tricuspid Regurgitation		
	Pearson	**95% Limits of agreement**	**ICC**	**Pearson**	**95% Limits of agreement**	**ICC**
Regurgitant flow volume (L/min)						
Interobserver						
Direct	0.929	(−1.56, 1.44)	0.935	0.992	(−1.32, 1.48)	0.985
Indirect	0.877	(−1.10, 1.50)	0.873	0.994	(−1.78, 0.83)	0.984
Intraobserver (direct)						
Reader 1	0.988	(−0.73, 0.61)	0.988	0.999	(−0.84, 0.52)	0.998
Reader 2	0.986	(−0.73, 0.68)	0.986	0.998	(−0.63, 0.47)	0.998
Regurgitant fraction (%)						
Interobserver						
Direct	0.861	(−16.0, 15.3)	0.870	0.975	(8.59, 9.70)	0.977
Indirect	0.838	(−14.6, 19.5)	0.769	0.968	(−22.1, 11.9)	0.902
Intraobserver (direct)						
Reader 1	0.983	(−6.37, 5.51)	0.984	0.995	(−4.97, 3.15)	0.995
Reader 2	0.976	(−8.53, 6.79)	0.974	0.992	(−5.34, 4.62)	0.993
Regurgitant volume (ml/beat)						
Interobserver						
Direct	0.909	(−26.6, 22.4)	0.913	0.990	(−19.9, 25.0)	0.982
Indirect	0.871	(−20.3, 25.1)	0.845	0.985	(−31.0, 14.8)	0.962
Intraobserver (direct)						
Reader 1	0.988	(−9.82, 8.49)	0.989	0.998	(−10.90, 6.90)	0.997
Reader 2	0.985	(−10.9, 10.4)	0.986	0.998	(−8.72, 6.35)	0.998

Data in parentheses are Bland-Altman 95% limits of agreement.

ICC = interclass correlation coefficient, 2-way random effects absolute agreement model.